

Late-time behavior of massive Dirac fields in a Schwarzschild background

Jiliang Jing*

*Institute of Physics and Department of Physics,
Hunan Normal University,
Changsha, Hunan 410081, P. R. China*

The late-time tail behavior of massive Dirac fields is investigated in the Schwarzschild black-hole geometry and the result is compared with that of the massive scalar fields. It is shown that in the intermediate late times there are three kinds of differences between the massive Dirac and scalar fields, (I) the asymptotic behavior of massive Dirac fields is dominated by a decaying tail without any oscillation, but the massive scalar field by a oscillatory inverse power-law decaying tail, (II) the dumping exponent for the massive Dirac field depends not only on the multiple number of the wave mode but also on the mass of the Dirac field, while that for the massive scalar field depends on the multiple number only, and (III) the decay of the massive Dirac field is slower than that of the massive scalar field.

PACS numbers: 03.65.Pm, 04.30.Nk, 04.70.Bw, 97.60.Lf

I. INTRODUCTION

The dynamical physical mechanism responsible for the relaxation of perturbation fields outside a black hole and the decay rates of the various perturbations have been extensively studied [1]-[19] since Wheeler introduced the no-hair theorem in the early 1970s [20, 21]. The massless neutral external perturbations were first studied by Price, and it was found that the late-time behavior for a fixed r is dominated by the factor $t^{-(2l+3)}$ for each multiple moment l [1]. The massless charged scalar field was studied in Refs. [2]-[3] and the conclusion was that a charged hair decay slower than a neutral one, i.e., the charged scalar hair outside a charged black hole is dominated by a $t^{-(2l+2)}$ tail. The massless late-time tail for the gravitational, electromagnetic, neutrino and scalar perturbations had also been considered in the case of the Kerr black holes in Refs. [4]-[6]. On the other hand, many authors found that the analysis of massive fields is also physically important since massive fields can cause interesting phenomena which are qualitatively different from the massless case. The evolution of a massive scalar field in the Schwarzschild background was analyzed by Starobinskii and Novikov [7], and they found that, because of the mass term, there are poles in the complex plane closer to the real axis than in the massless case, which leads to inverse power-law behavior with smaller indices than the massless case. Hod and Piran [8] pointed out that, if the field mass μ is small, namely $\mu M \ll 1$, the oscillatory inverse power-law behavior

$$\Phi \sim t^{-(l+3/2)} \sin(\mu t), \quad (1.1)$$

dominates as the intermediate late-time tails in the Reissner-Nordström background. We [9] recently investigated the late-time tails of the massless and the self-interacting (massive) scalar fields in a stationary axisymmetric Einstein-Maxwell-dilaton-axion black-hole geometry, and found that the dumping exponents is independent of the rotation parameter and the dilaton of the black hole.

Although much attention has been paid to the study of the late-time behaviors of the scalar, gravitational, electromagnetic in static and stationary black-hole backgrounds, however, to my best knowledge, at the moment the late-time evolution of the Dirac fields has not been investigated. The aim of this paper is to study the intermediate late-time tail behavior of the massive Dirac fields in the Schwarzschild black-hole background and to see whether or not special properties exist in this case.

The plan of the paper is as follows. In Sec.2 the decoupled massive Dirac equations in the Schwarzschild spacetime are presented. In Sec.3 the black-hole Green's function is introduced by using the spectral decomposition method [22]. In Sec.4 the intermediate late-time evolution of the Dirac massive fields in the Schwarzschild background

*Electronic address: jljing@hunnu.edu.cn

is investigated. The section V is devoted to a summary and conclusion. In the appendix we study whether the conclusions might change if the tortoise coordinate is defined in the conventional way.

II. DIRAC EQUATION IN THE SCHWARZSCHILD SPACETIME

Dirac equation in a general background spacetime can be expressed as [23]

$$[\gamma^a e_a^\mu (\partial_\mu + \Gamma_\mu) + \mu] \Psi = 0, \quad (2.1)$$

where μ is the mass of the Dirac field, γ^a is the Dirac matrix, e_a^μ is the inverse of the tetrad e_μ^a , and Γ_μ is the spin connection, which is defined as $\Gamma_\mu = \frac{1}{8}[\gamma^a, \gamma^b] e_a^\nu e_{b\nu;\mu}$. For the Schwarzschild black hole

$$ds^2 = -f dt^2 + \frac{1}{f} dr^2 + r^2(d\theta^2 + \sin^2\theta d\varphi^2), \quad (2.2)$$

with

$$f = 1 - \frac{2M}{r}, \quad (2.3)$$

where the parameters M represents the mass of the black hole, we can take the tetrad as

$$e_\mu^a = \text{diag}(\sqrt{f}, \frac{1}{\sqrt{f}}, r, r \sin\theta). \quad (2.4)$$

Introducing an ansatz

$$\Psi = f^{-\frac{1}{4}} \begin{pmatrix} \frac{iF_1^{(\pm)}(r,t)}{r} \phi_{jm}^\pm(\theta, \varphi) \\ \frac{F_2^{(\pm)}(r,t)}{r} \phi_{jm}^\mp(\theta, \varphi) \end{pmatrix}, \quad (2.5)$$

with

$$\phi_{jm}^+ = \begin{pmatrix} \sqrt{\frac{j+m}{2j}} Y_l^{m-1/2} \\ \sqrt{\frac{j-m}{2j}} Y_l^{m+1/2} \end{pmatrix} \quad \text{for } j = l + \frac{1}{2},$$

$$\phi_{jm}^- = \begin{pmatrix} \sqrt{\frac{j+1-m}{2j+2}} Y_l^{m-1/2} \\ -\sqrt{\frac{j+1+m}{2j+2}} Y_l^{m+1/2} \end{pmatrix} \quad \text{for } j = l - \frac{1}{2},$$

Cho [24] find that the cases for (+) and (-) in the functions F_1^\pm and F_2^\pm can be put together, and then the decoupled equations can be written as

$$\left(\frac{\partial^2}{\partial \hat{r}_*^2} - \frac{\partial^2}{\partial t^2} - V_i \right) F_i(\hat{r}_*, t) = 0, \quad i=1,2 \quad (2.6)$$

where

$$\hat{r}_* = r + 2M \ln \left(\frac{r}{2M} - 1 \right) + \frac{1}{2\omega} \tan^{-1} \left(\frac{\mu r}{|k|} \right) \quad (2.7)$$

$$V_{1,2} = \pm \frac{dW}{d\hat{r}_*} + W^2, \quad (2.8)$$

with

$$W = \frac{\Delta^{1/2}(k^2 + \mu^2 r^2)^{3/2}}{r^2(k^2 + \mu^2 r^2) + \mu k \Delta / 2\omega}, \quad (2.9)$$

where $\Delta = r(r - 2M)$. Here k goes over all positive and negative integers. Positive integers represent the (+) case of Eq. (2.8) with $k = j + 1/2$ and $j = l + 1/2$, while negative integers represent the (-) case of Eq. (2.8) with $k = -(j + 1/2)$ and $j = l - 1/2$. Equation (2.8) shows that the potentials V_1 and V_2 are related to the metric function \sqrt{f} which differs from potentials for the scalar, electromagnetic and gravitational fields [25, 26]. We will use the potential (2.8) to study the late-time tail behavior of the massive Dirac fields in the Schwarzschild black-hole geometry.

It is easy to see that near the event horizon the effective potential $V_{1,2}$ becomes zero. Then the radial asymptotic solutions can be expressed as

$$R_i \simeq e^{\pm i\omega \hat{r}_*} = e^{\pm i\omega r_*} e^{\pm \frac{i}{2} \tan^{-1}\left(\frac{\mu r}{|k|}\right)}, \quad (2.10)$$

where $r_* = \int 1/f dr$ is the usual tortoise coordinate. By comparing Eq. (2.10) with the scalar field solutions $e^{\pm i\omega r_*}$ [8] we know that the Dirac field possesses a additional factor $e^{\pm \frac{i}{2} \tan^{-1}\left(\frac{\mu r}{|k|}\right)}$. The appearance of the factor seems due to we used the ‘‘tortoise’’ coordinate (2.7). However, the factor still exists even if we use the usual tortoise coordinate (see appendix for detail).

III. THE BLACK HOLE GREEN’S FUNCTION

It is well known that the time evolution of a wave field $\Psi(r_*, t)$ follows from

$$\Psi(r_*, t) = \int [G(r_*, r'_*; t) \partial_t \Psi(r'_*, 0) + \partial_t G(r_*, r'_*; t) \Psi(r'_*, 0)] dr'_*, \quad (3.1)$$

where the black-hole (retarded) Green’s function $G(r_*, r'_*; t)$ is defined by

$$\left[\frac{\partial^2}{\partial t^2} - \frac{\partial^2}{\partial r_*^2} + V(r) \right] G(r_*, r'_*; t) = \delta(t) \delta(r_* - r'_*). \quad (3.2)$$

The causality condition gives us the initial condition $G(r_*, r'_*; t) = 0$ for $t \leq 0$. In order to get $G(r_*, r'_*; t)$ we use the Fourier transform

$$\tilde{G}(r_*, r'_*; \omega) = \int_{0^-}^{\infty} G(r_*, r'_*; t) e^{i\omega t} dt. \quad (3.3)$$

The Fourier transform is analytic in the upper half ω -plane, and the corresponding inversion formula is given by

$$G(r_*, r'_*; t) = \frac{1}{2\pi} \int_{-\infty+ic}^{\infty+ic} \tilde{G}(r_*, r'_*; \omega) e^{-i\omega t} d\omega, \quad (3.4)$$

where c is some positive constant.

We define two auxiliary functions $\tilde{\Psi}_1(r_*, \omega)$ and $\tilde{\Psi}_2(r_*, \omega)$ which are (linearly independent) solutions to the homogeneous equation

$$\left[\frac{d^2}{dr_*^2} + \omega^2 - V(r) \right] \tilde{\Psi}_i(r_*, \omega) = 0, \quad i = 1, 2. \quad (3.5)$$

Let the Wronskian be

$$W(\omega) = W(\tilde{\Psi}_1, \tilde{\Psi}_2) = \tilde{\Psi}_1 \tilde{\Psi}_{2,x} - \tilde{\Psi}_2 \tilde{\Psi}_{1,x}, \quad (3.6)$$

and using the two solutions $\tilde{\Psi}_1$ and $\tilde{\Psi}_2$, the black-hole Green’s function can be constructed as

$$\tilde{G}_l(r_*, r'_*; \omega) = -\frac{1}{W(\omega)} \begin{cases} \tilde{\Psi}_1(r_*, \omega) \tilde{\Psi}_2(r'_*, \omega), & r_* < r'_*; \\ \tilde{\Psi}_1(r'_*, \omega) \tilde{\Psi}_2(r_*, \omega), & r_* > r'_*. \end{cases} \quad (3.7)$$

IV. LATE-TIME TAILS OF THE MASSIVE DIRAC FIELDS

It is well known that massive tails exist even in a flat spacetime [27]. This phenomenon is related to the fact that different frequencies forming a massive wave packet have different phase velocities. One will see that at intermediate times the backscattering from asymptotically far regions (which dominates the tails of massless fields) is negligible compared to the flat spacetime massive tails that appear here. Hod, Piran, and Leaver [8, 22] argued that the asymptotic massive tail is associated with the existence of a branch cut (in $\tilde{\Psi}_2$) placed along the interval $-\mu \leq \omega \leq \mu$. This tail arises from the integral of the Green function $\tilde{G}(r_*, r'_*; \omega)$ around the branch (denoted by $G^C(r_*, r'_*; \omega)$). So our goal is to evaluate $G^C(r_*, r'_*; \omega)$.

Now we assume that both the observer and the initial data are situated far away from the black hole so that $r \gg M$. One may expand the wave-equation (3.5) with the potential V_1 which is given by (2.8) (or V_2) for the massive Dirac field as a power series in M/r (neglecting terms of order $O((M/r)^2)$) as follows

$$\left(\frac{d^2}{dr^2} + \omega^2 - \mu^2 + \frac{4M\omega^2 - 2M\mu^2}{r} - \frac{k^2 - k\omega/\mu}{r^2} \right) \xi(r, \omega) = 0, \quad (4.1)$$

with

$$\xi = (1 - 2M/r)^{1/2} \left[1 + \left(1 - \frac{2M}{r} \right) \frac{\mu|k|}{2\omega(k^2 + \mu^2 r^2)} \right]^{-1/2} \tilde{\Psi}. \quad (4.2)$$

At great distances, the only difference between effective potentials of the scalar and Dirac fields is that the term $l(l+1)/r^2$ for the massive scalar field is now replaced by $(k^2 - k\omega/\mu)/r^2$ for the massive Dirac field. As we will see later, it is the difference that leads to new result.

Let us introduce

$$z = 2\sqrt{\mu^2 - \omega^2}r = 2\varpi r \quad (4.3)$$

$$\xi = e^{-z/2} z^{1/2+b} \Phi, \quad (4.4)$$

$$b^2 = \frac{1}{4} + k^2 - \frac{k\omega}{\mu}, \quad (4.5)$$

$$a = \frac{M\mu^2}{\varpi} - 2M\varpi. \quad (4.6)$$

Then Eq. (4.1) becomes the confluent hypergeometric equation

$$z \frac{d^2 \Phi}{dz^2} + (1 + 2b - z) \frac{d\Phi}{dz} - \left(\frac{1}{2} + b - a \right) \Phi = 0. \quad (4.7)$$

It follows that two basic solutions required in order to build the Green's function can be expressed as

$$\tilde{\psi}_1 = Ae^{-\varpi r} (2\varpi r)^{1/2+b} M(1/2 + b - a, 1 + 2b, 2\varpi r), \quad (4.8)$$

$$\tilde{\psi}_2 = Be^{-\varpi r} (2\varpi r)^{1/2+b} U(1/2 + b - a, 1 + 2b, 2\varpi r), \quad (4.9)$$

where A and B are normalization constants. The functions $M(\tilde{a}, \tilde{b}, z)$ and $U(\tilde{a}, \tilde{b}, z)$ represent the two standard solutions to the confluent hypergeometric equation [28]. $U(\tilde{a}, \tilde{b}, z)$ is a many-valued function, i.e., there is a cut in $\tilde{\psi}_2$.

Using Eq. (3.4), one finds that the branch cut contribution to the Green's function is described by

$$\begin{aligned} G^C(r_*, r'_*, t) &= \frac{1}{2\pi} \int_{-\mu}^{\mu} \left[\frac{\tilde{\psi}_1(r'_*, \omega e^{i\pi}) \tilde{\psi}_2(r_*, \omega e^{i\pi})}{W(\omega e^{i\pi})} - \frac{\tilde{\psi}_1(r'_*, \omega) \tilde{\psi}_2(r_*, \omega)}{W(\omega)} \right] e^{-i\omega t} d\omega \\ &= \frac{1}{2\pi} \int_{-\mu}^{\mu} F(\varpi) e^{-i\omega t} d\omega. \end{aligned} \quad (4.10)$$

Using the following relations

$$\begin{aligned} \tilde{\psi}_1(2\varpi r e^{i\pi}) &= Ae^{(1/2+b)i\pi} e^{-\varpi r} (2\varpi r)^{1/2+b} M(1/2 + b + a, 1 + 2b, 2\varpi r), \\ \tilde{\psi}_2(2\varpi r) &= B \frac{\Gamma(-2b)}{\Gamma(1/2 - b - a)} e^{-\varpi r} (2\varpi r)^{1/2+b} M(1/2 + b - a, 1 + 2b, 2\varpi r) \\ &\quad + B \frac{\Gamma(2b)}{\Gamma(1/2 + b - a)} e^{-\varpi r} (2\varpi r)^{1/2-b} M(1/2 - b - a, 1 - 2b, 2\varpi r), \end{aligned} \quad (4.11)$$

we find

$$W(\varpi e^{i\pi}) = -W(\varpi) = AB \frac{\Gamma(2b)}{\Gamma(1/2 + b - a)} 4b\varpi. \quad (4.12)$$

and

$$\begin{aligned} F(\varpi) &= \frac{(r_*)^{\frac{1}{2}-b}(r'_*)^{\frac{1}{2}+b}e^{-\varpi(r_*+r'_*)}}{2b} \left[M\left(\frac{1}{2} + b + a, 1 + 2b, 2\varpi r'_*\right) M\left(\frac{1}{2} - b + a, 1 - 2b, 2\varpi r_*\right) \right. \\ &\quad \left. - M\left(\frac{1}{2} + b - a, 1 + 2b, 2\varpi r'_*\right) M\left(\frac{1}{2} - b - a, 1 - 2b, 2\varpi r_*\right) \right] - \frac{\Gamma(-2b)\Gamma(\frac{1}{2} + b - a)}{\Gamma(2b)\Gamma(\frac{1}{2} - b - a)} \\ &\quad \times \frac{(4\varpi^2 r_* r'_*)^{\frac{1}{2}+b}e^{-\varpi(r_*+r'_*)}}{4\varpi b} \left[M\left(\frac{1}{2} + b - a, 1 + 2b, 2\varpi r'_*\right) M\left(\frac{1}{2} + b - a, 1 + 2b, 2\varpi r_*\right) \right. \\ &\quad \left. + e^{(1+2b)i\pi} M\left(\frac{1}{2} + b + a, 1 + 2b, 2\varpi r'_*\right) M\left(\frac{1}{2} + b + a, 1 + 2b, 2\varpi r_*\right) \right]. \end{aligned} \quad (4.13)$$

If we further assume that both the observer and the initial data are situated in the region $M \ll r \ll M/(\mu M)^2$ and we are interested in the intermediate asymptotic behavior of the Dirac field [$M \ll r \ll t \ll M/(M\mu)^2$], we find that the frequency range $\varpi = O(\sqrt{\mu/t})$, which gives the dominant contribution to the integral, implies $a \ll 1$. Eq. (4.1) shows that a originates from the $1/r$ term which describes the effect of backscattering off the spacetime curvature. Thus, the backscattering off the curvature from the asymptotically regions is negligible for the case $a \ll 1$. So, we get

$$\begin{aligned} F(\varpi) &\approx -\frac{\Gamma(-2b)\Gamma(\frac{1}{2} + b)}{\Gamma(2b)\Gamma(\frac{1}{2} - b)} \frac{(2\varpi r_*)^{1/2+b}(2\varpi r'_*)^{1/2+b}e^{-\varpi(r_*+r'_*)}}{4\varpi b} \\ &\quad (1 + e^{(1+2b)i\pi}) M\left(\frac{1}{2} + b, 1 + 2b, 2\varpi r'_*\right) M\left(\frac{1}{2} + b, 1 + 2b, 2\varpi r_*\right). \end{aligned} \quad (4.14)$$

Noticing that $M(\tilde{a}, \tilde{b}, z) \approx 1$ as $z \rightarrow 0$, we have

$$\begin{aligned} F(\varpi) &\approx -\frac{1 + e^{(1+2b)i\pi}}{4\varpi b} \frac{\Gamma(-2b)\Gamma(\frac{1}{2} + b)}{\Gamma(2b)\Gamma(\frac{1}{2} - b)} (2\varpi)^{1+2b} (r_* r'_*)^{1/2+b} \\ &= \frac{\pi}{\sin(\pi b)} \frac{1 + e^{(1+2b)i\pi}}{2^{1+2b} b^2} \frac{\varpi^{2b}}{\Gamma(b)^2} (r_* r'_*)^{1/2+b}, \end{aligned} \quad (4.15)$$

where we used the formulae $\Gamma(2z) = \frac{1}{\sqrt{2\pi}} 2^{2z-1/2} \Gamma(z)\Gamma(1/2+z)$ and $\Gamma(-z) = -\frac{\pi}{\sin(\pi z)} \frac{1}{z\Gamma(z)}$. Substituting Eq. (4.15) into the Eq. (4.10), we obtain

$$G^C(r_*, r'_*, t) = \frac{1}{4} \int_{-\mu}^{\mu} \frac{1}{\sin(\pi b)} \frac{1 + e^{(1+2b)i\pi}}{2^{2b} b^2} \frac{(r_* r'_*)^{1/2+b}}{\Gamma(b)^2} (\mu^2 - \omega^2)^b e^{-i\omega t} d\omega. \quad (4.16)$$

Unfortunately, the integral can not be evaluated analytically since the parameter $b = \sqrt{1/4 + k^2 - k\omega/\mu}$ depends on ω . However, we can work out the integral numerically and the results are presented in figures 1-3 with the form $\ln |G^C(r_*, r'_*, t)|$ versus t . Figure 1 describes different k with the same mass ($\mu = 0.01$), which shows that the dumping exponent depends on the multiple number of the wave mode. Figure 2 gives different mass μ with the same multiple number ($k = 1$), which indicates that the dumping exponent depends on the mass μ of the Dirac fields. In Fig. 3 the lines (a) represent the result of the Green function (4.16) of the massive Dirac field with different k , and lines (b) show the corresponding result of the massive scalar field. We learn from Fig. 3 that late-time behavior of massive Dirac fields is dominated by a decaying tail without any oscillation, and the decay of the massive Dirac field is slower than that of the massive scalar field.

V. SUMMARY AND DISCUSSIONS

We have studied the intermediate late-time tail behavior of massive Dirac fields in the Schwarzschild black-hole geometry and the result is compared with that of the massive scalar fields. We know from the figures that there are three differences between the massive Dirac and scalar fields due to the fact that the parameter $b = \sqrt{1/4 + k^2 - k\omega/\mu}$

is related to ω for the massive Dirac fields while $b = l + 1/2$ for the massive scalar fields, (I) the late-time behavior of massive Dirac fields is dominated by an inverse power-law decaying tail without any oscillation, but the massive scalar field by an oscillatory decaying tail, (II) the dumping exponent (i.e., α in term $1/t^\alpha$) for the massive Dirac field depends not only on the multiple number of the wave mode but also on the mass of the Dirac field, while $\alpha = (l + 3/2)$ for the massive scalar field depends on the multiple number only, and (III) the decay of the massive Dirac field is slower than that of the massive scalar field.

Acknowledgments

This work was supported in part by the National Natural Science Foundation of China under Grant No. 10275024; the FANEDD under Grant No. 200317; the Hunan Provincial Natural Science Foundation of China under Grant No. 04JJ3019; and the National Basic Research program of China under grant No. 2003CB716300.

APPENDIX A: MAY THE CONCLUSIONS CHANGE IN THE USUAL TORTOISE COORDINATES?

The ‘‘tortoise’’ coordinate (2.7) is a function of the background geometry and the test field, which is different from the usual tortoise one, $r_* = \int \frac{dr}{f}$. Might the conclusions of this paper change if we use usual tortoise coordinate instead of the coordinate (2.7)? In the appendix we will address this question.

The Dirac equations are given by [29]

$$\begin{aligned}\sqrt{2}\nabla_{BB'}P^B + i\mu\bar{Q}_{B'} &= 0, \\ \sqrt{2}\nabla_{BB'}Q^B + i\mu\bar{P}_{B'} &= 0,\end{aligned}\tag{A1}$$

where $\nabla_{BB'}$ is covariant differentiation, $A_{BB'}$ is the electromagnetic field potential, P^B and Q^B are the two-component spinors, and μ is the particle mass. In the Newman-Penrose formalism [30] the equations become

$$\begin{aligned}(D + \epsilon - \rho)P^0 + (\bar{\delta} + \pi - \alpha)P^1 &= 2^{-1/2}i\mu\bar{Q}^{1'}, \\ (\Delta + \mu - \gamma)P^1 + (\delta + \beta - \tau)P^0 &= -2^{-1/2}i\mu\bar{Q}^{0'}, \\ (D + \bar{\epsilon} - \bar{\rho})\bar{Q}^{0'} + (\delta + \bar{\pi} - \bar{\alpha})\bar{Q}^{1'} &= -2^{-1/2}i\mu P^1, \\ (\Delta + \bar{\mu} - \bar{\gamma})\bar{Q}^{1'} + (\bar{\delta} + \bar{\beta} - \bar{\tau})\bar{Q}^{0'} &= 2^{-1/2}i\mu P^0,\end{aligned}\tag{A2}$$

For the Schwarzschild spacetime the null tetrad can be taken as

$$\begin{aligned}l^\mu &= \left(\frac{r^2}{\Delta}, 0, 0, 0\right), \\ n^\mu &= \frac{1}{2}\left(1, -\frac{\Delta}{r^2}, 0, 0\right) \\ m^\mu &= \frac{1}{\sqrt{2}r}\left(0, 0, 1, \frac{i}{\sin\theta}\right),\end{aligned}\tag{A3}$$

Then, if we set

$$\begin{aligned}P^0 &= \frac{1}{r}f_1(r, \theta)e^{-i(\omega t - m\varphi)}, \\ P^1 &= f_2(r, \theta)e^{-i(\omega t - m\varphi)}, \\ \bar{Q}^{1'} &= g_1(r, \theta)e^{-i(\omega t - m\varphi)}, \\ \bar{Q}^{0'} &= -\frac{1}{r}g_2(r, \theta)e^{-i(\omega t - m\varphi)},\end{aligned}\tag{A4}$$

where ω and m are the energy and angular momentum of the Dirac particles, Eq. (A2) can be simplified as

$$\begin{aligned}
\mathcal{D}_0 f_1 + \frac{1}{\sqrt{2}} \mathcal{L}_{1/2} f_2 &= \frac{1}{\sqrt{2}} i\mu r g_1, \\
\Delta \mathcal{D}_{1/2}^\dagger f_2 - \sqrt{2} \mathcal{L}_{1/2}^\dagger f_1 &= -\sqrt{2} i\mu r g_1, \\
\mathcal{D}_0 g_2 - \frac{1}{\sqrt{2}} \mathcal{L}_{1/2}^\dagger g_1 &= \frac{1}{\sqrt{2}} i\mu r f_2, \\
\Delta \mathcal{D}_{1/2}^\dagger g_1 + \sqrt{2} \mathcal{L}_{1/2} g_2 &= -\sqrt{2} i\mu r f_1,
\end{aligned} \tag{A5}$$

with

$$\begin{aligned}
\mathcal{D}_n &= \frac{\partial}{\partial r} - \frac{iK}{\Delta} + 2n \frac{r-M}{\Delta}, \\
\mathcal{D}_n^\dagger &= \frac{\partial}{\partial r} + \frac{iK}{\Delta} + 2n \frac{r-M}{\Delta}, \\
\mathcal{L}_n &= \frac{\partial}{\partial \theta} + \frac{m}{\sin \theta} + n \cot \theta, \\
\mathcal{L}_n^\dagger &= \frac{\partial}{\partial \theta} - \frac{m}{\sin \theta} + n \cot \theta, \\
K &= r^2 \omega.
\end{aligned} \tag{A6}$$

It is now apparent that the variables can be separated by the substitutions

$$\begin{aligned}
f_1 &= R_{-1/2}(r) S_{-1/2}(\theta), \\
f_2 &= R_{+1/2}(r) S_{+1/2}(\theta), \\
g_1 &= R_{+1/2}(r) S_{-1/2}(\theta), \\
g_2 &= R_{-1/2}(r) S_{+1/2}(\theta).
\end{aligned} \tag{A7}$$

Thus, we have[31]

$$\left[\Delta \mathcal{D}_{1/2}^\dagger \mathcal{D}_0 - \frac{i\mu\Delta}{\lambda + i\mu r} \mathcal{D}_0 - (\lambda^2 + \mu^2 r^2) \right] R_{-1/2} = 0, \tag{A8}$$

and $\sqrt{\Delta} R_{+1/2}$ satisfies the complex-conjugate equation. The decoupled equations can then be explicitly expressed as

$$\sqrt{\Delta} \frac{d}{dr} \left(\sqrt{\Delta} \frac{dR_{-1/2}}{dr} \right) - \frac{i\mu\Delta}{\lambda + i\mu r} \frac{dR_{-1/2}}{dr} + P_- R_{-1/2} = 0, \tag{A9}$$

$$\frac{1}{\sqrt{\Delta}} \frac{d}{dr} \left(\Delta^{3/2} \frac{dR_{+1/2}}{dr} \right) + \frac{i\mu\Delta}{\lambda - i\mu r} \frac{dR_{+1/2}}{dr} + P_+ R_{+1/2} = 0, \tag{A10}$$

with

$$P_- = \frac{K^2 + i(r-M)K}{\Delta} - 2i\omega r - \frac{\mu K}{\lambda + i\mu r} - \mu^2 r^2 - \lambda^2, \tag{A11}$$

$$P_+ = \frac{K^2 - i(r-M)K}{\Delta} + 2i\omega r + 2s + \frac{\mu(i(r-M) - K)}{\lambda - i\mu r} - \mu^2 r^2 - \lambda^2, \tag{A12}$$

where $\lambda^2 = (l-s)(l+s+1)$ is the separation constant. Introducing an usual tortoise coordinate

$$r_* = \int \frac{r^2}{\Delta} dr, \tag{A13}$$

and resolving Eqs. (A9) and (A10) in the form

$$\begin{aligned}
R_{+1/2} &= \frac{\Delta^{-1/4}}{r} (\lambda^2 + \mu^2 r^2)^{1/4} e^{-i\vartheta/2} \Psi_+, \\
R_{-1/2} &= \frac{\Delta^{1/4}}{r} (\lambda^2 + \mu^2 r^2)^{1/4} e^{i\vartheta/2} \Psi_-,
\end{aligned} \tag{A14}$$

with

$$\vartheta = \arctan(\mu r/\lambda), \quad (\text{A15})$$

we obtain two wave-equations

$$\frac{d^2\Psi_+}{dr_*^2} + \left\{ \frac{dH_+}{dr_*} - H_+^2 + \frac{\Delta}{r^4} P_+ \right\} \Psi_+ = 0, \quad (\text{A16})$$

$$\frac{d^2\Psi_-}{dr_*^2} + \left\{ \frac{dH_-}{dr_*} - H_-^2 + \frac{\Delta}{r^4} P_- \right\} \Psi_- = 0, \quad (\text{A17})$$

where

$$H_- = \frac{1}{4r^2} \frac{d\Delta}{dr} - \frac{\Delta}{r^3} + \frac{i\mu}{2(\lambda + i\mu r)} \frac{\Delta}{r^2}, \quad (\text{A18})$$

$$H_+ = - \left[\frac{1}{4r^2} \frac{d\Delta}{dr} + \frac{\Delta}{r^3} + \frac{i\mu}{2(\lambda - i\mu r)} \frac{\Delta}{r^2} \right]. \quad (\text{A19})$$

Near the event horizon the asymptotic solutions are

$$R_{\pm 1/2} \simeq e^{i\omega r_*} e^{\mp \frac{i}{2} \tan^{-1}(\frac{\mu r}{\lambda})}, \quad \text{or} \quad R_{\pm 1/2} \simeq \Delta^{-s} e^{-i\omega r_*} e^{\pm \frac{i}{2} \tan^{-1}(\frac{\mu r}{\lambda})}. \quad (\text{A20})$$

One may expand the wave-equations (A16) and (A17) as a power series in M/r (neglecting terms of order $O((M/r)^2)$) as follows

$$\left[\frac{d^2}{dr^2} + \omega^2 - \mu^2 + \frac{4M\omega^2 - 2M\mu^2}{r} - \frac{\lambda^2 + \frac{\lambda}{\mu}\omega}{r^2} \right] \xi_{\pm} = 0, \quad (\text{A21})$$

where $\xi_{\pm} = (1 - 2M/r)^{1/2} \Psi_{\pm}$. It is of interesting to note that Eq. (A21) becomes Eq. (4.1) if we replace λ by $-k$, which shows that the conclusions of this paper do not change if we use usual tortoise coordinate instead of the coordinate (2.7).

-
- [1] R. H. Price, Phys. Rev. D 5, 2419 (1972).
 - [2] S. Hod and T. Piran, Phys. Rev. D 58, 024017 (1998).
 - [3] S. Hod and T. Piran, Phys. Rev. D 58, 024019 (1998).
 - [4] L. Barack and A. Ori, Phys. Rev. Lett. 82, 4388 (1999).
 - [5] S. Hod, Phys. Rev. Lett. 84, 10 (2000).
 - [6] S. Hod, Phys. Rev. D 58, 104022 (1998).
 - [7] A. A. Starobinskii and I. D. Novikov (unpublished).
 - [8] S. Hod and T. Piran, Phys. Rev. D 58, 044018 (1998).
 - [9] Qiyuan Pan and Jiliang Jing, Chinese Physics, to be published.
 - [10] J. Karkowski, Z. Swierczynski, and E. Malec, gr-qc/0303101.
 - [11] H. Koyama and A. Tomimatsu, Phys. Rev. D 64, 044014 (2001).
 - [12] N. Andersson, Phys. Rev. D 55, 468 (1997).
 - [13] Vitor Cardoso, Shijun Yoshida, Oscar J.C. Dias, and Jose P.S. Lemos, Phys. Rev. D 68, 061503 (2003).
 - [14] Hongwei Yu, Phys. Rev. D 65, 087502 (2002).
 - [15] L. M. Burko and A. Ori, Phys. Rev. D 56, 7820 (1997).
 - [16] L. M. Burko and G. Khanna, gr-qc/0403018 (2004).
 - [17] C. Gundlach, R. H. Price, and J. Pullin, Phys. Rev. D 49, 890 (1994).
 - [18] M. A. Scheel, A. L. Erickcek, L. M. Burko, L. E. Kidder, H. P. Pfeiffer, and S. A. Teukolsky, Phys. Rev. D 69, 104006 (2004).
 - [19] E. S. C. Ching, P. T. Leung, W. M. Suen, and K. Young, Phys. Rev. D 52, 2118 (1995).
 - [20] R. Ruffini and J. A. Wheeler, Phys. Today 24 (1), 30 (1971).
 - [21] C. W. Misner, K. S. Thorne, and J. A. Wheeler, Gravitation (Freeman, San Francisco, 1973).
 - [22] E. W. Leaver, Phys. Rev. D 34, 384 (1986).
 - [23] D. R. Brill and J. A. Wheeler, Rev. Mod. Phys. 29, 465 (1957);
 - [24] H. T. Cho, Phys. rev. D 68, 024003 (2003).

- [25] Jiliang Jing, Phys. Rev. D 69 084009 (2004).
- [26] M. Giammatteo and Jiliang Jing gr-qc/0403030 (2004).
- [27] P. M. Morse and H. Feshbach, Methods of Theoretical Physics (McGraw-Hill, New York, 1953).
- [28] M. Abramowitz and I. A. Stegun, Handbook of Mathematical Functions (Dover, New York, 1970).
- [29] D. N. Page, Phys. Rev. D 14, 1509 (1976).
- [30] E. Newman and R. Penrose, J. Math. Phys. (N. Y.) 3, 566 (1962).
- [31] S. Chandrasekhar, The mathematical theory of black holes, p546 (Oxford University Press, New York, 1992).

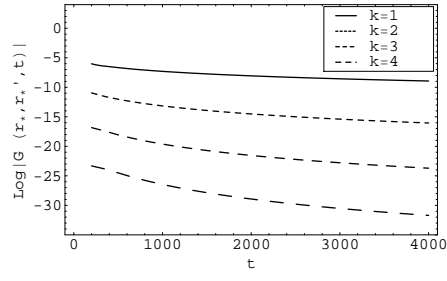


FIG. 1: The figure describes $\ln|G^C(r_*, r'_*, t)|$ versus t for different k with the same mass ($\mu = 0.01$), which shows that the dumping exponent depends on the multiple number of the wave mode.

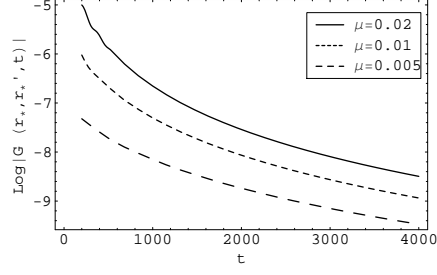


FIG. 2: The figure describes $\ln|G^C(r_*, r'_*, t)|$ versus t for different mass μ with the same multiple number ($k = 1$), which indicates that the dumping exponent depends on the mass μ of the Dirac fields.

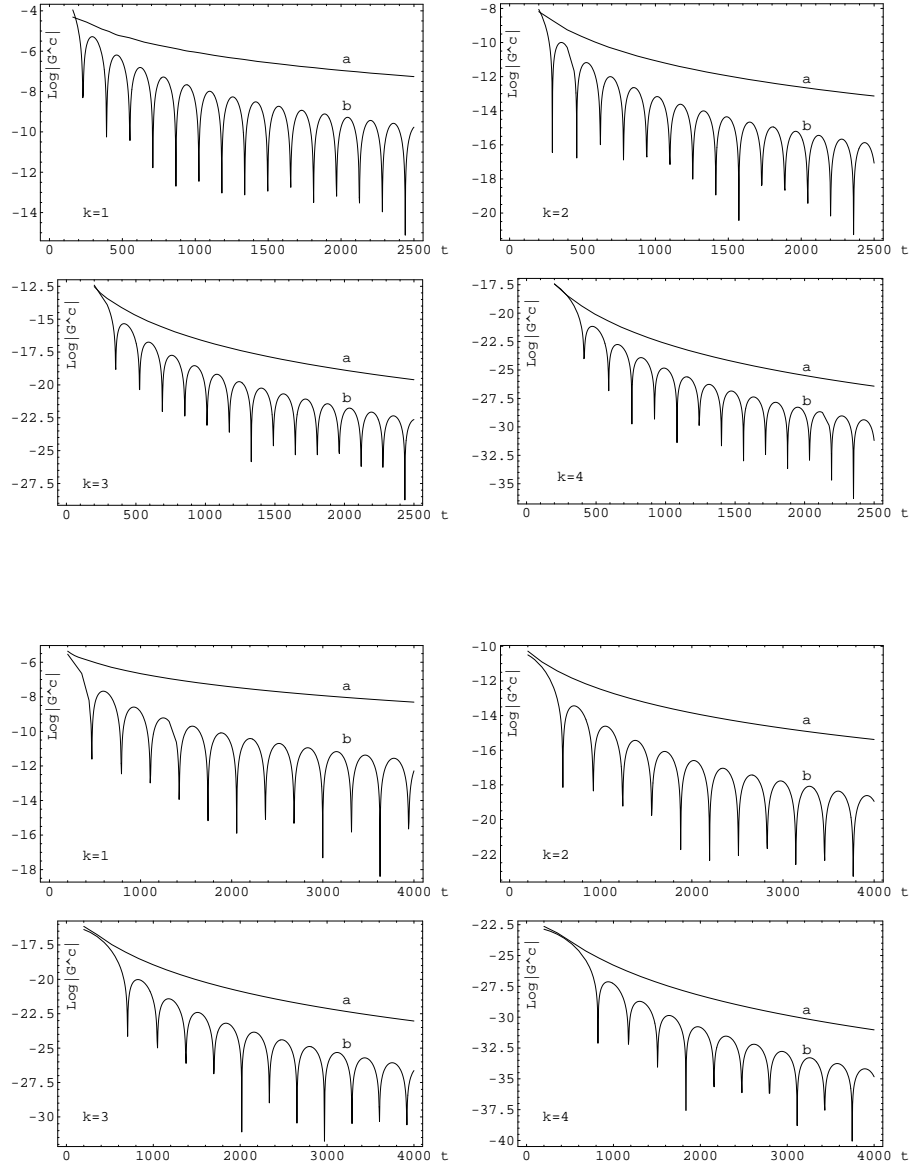


FIG. 3: The above four figures describe $\ln |G^C(r_*, r'_*, t)|$ versus t for $\mu = 0.02$, and below four for $\mu = 0.01$. The dashed lines represent the result of the Green function of the massive Dirac field with different k . For comparing, we also show the corresponding result of the Scalar field with solid lines. It is shown that the late-time behavior of massive Dirac fields is dominated by a decaying tail without any oscillation, and the decay of the massive Dirac field is slower than that of the massive scalar field.